Essential Iris Atrophy, Pigment Dispersion, and Glaucoma in DBA/2J Mice

Simon W. M. John,[1,2,3] *Richard S. Smith,*[1,2] *Olga V. Savinova,*[1] *Norman L. Hawes,*[1] *Bo Chang,*[1] *Dan Turnbull,*[4] *Muriel Davisson,*[1] *Thomas H. Roderick,*[1] *and John R. Heckenlively*[5]

Purpose. To characterize ocular abnormalities associated with iris atrophy in DBA/2J mice and to determine whether mice of this strain develop elevated intraocular pressure (IOP) and glaucoma.

Methods. Different approaches, including slit-lamp biomicroscopy, ophthalmoscopic examination, ultrasound backscatter microscopy, and histology were used to examine the eyes of DBA/2J mice ranging from 2 to 30 months old. IOP was measured in DBA/2J mice of different ages.

Results. DBA/2J mice were found to develop pigment dispersion, iris transillumination, iris atrophy, anterior synechias, and elevated IOP. IOP was elevated in most mice by the age of 9 months. These changes were followed by the death of retinal ganglion cells, optic nerve atrophy, and optic nerve cupping. The prevalence and severity of these lesions increased with age. Optic nerve atrophy and optic nerve cupping was present in the majority of mice by the age of 22 months.

Conclusions. DBA/2J mice develop a progressive form of secondary angle-closure glaucoma that appears to be initiated by iris atrophy and the associated formation of synechias. This mouse strain represents a useful model to evaluate mechanisms of pressure-related ganglion cell death and optic nerve atrophy, and to evaluate strategies for neuroprotection. (*Invest Ophthalmol Vis Sci.* 1998;39: 951-962)

Glaucoma accounts for 15% of blindness worldwide[1] and is a leading cause of blindness in the United States.[2] It is the outcome of complex disease processes involving the loss of retinal ganglion cells and their nerve fibers. This loss produces a characteristic excavation or cupping of the optic nerve head. Many forms of glaucoma exist.[3] The most common is adult-onset, primary open-angle glaucoma.[4]

Glaucoma is usually associated with high intraocular pressure (IOP) that results from an increased resistance to drainage of the aqueous humor.[5] However, besides elevated IOP, there are other important factors that modify susceptibility to glaucoma. Nerve damage does not develop in many persons who have high IOP, whereas in others nerve damage develops despite IOP levels in the normal range.[2] Recent advances in understanding glaucoma include the association of various chromosomal loci with different forms of glaucoma[6] and the identification of specific mutant genes that cause juvenile-onset, open-angle glaucoma[7] and primary congenital glaucoma.[8] Despite these advances, the genetic and environmental factors causing and modifying glaucoma phenotypes in most families are not clearly defined.[6]

Though important, studies of the pathologic causes of glaucoma in human eyes are difficult to interpret. This is because most ocular samples are unavailable until years of elevated IOP and years of treatment with various drugs, surgeries, or both have had their own effects. The primary changes that initiated glaucoma may be obscured. Consequently, relatively little is known about the pathophysiological mechanisms involved in the early stages of any type of glaucoma.

Genetic studies in mice are proving to be a powerful means to learn about genes and pathologic mechanisms that cause disease or alter disease susceptibility.[9] Laboratory mice live for approximately 2 years and often develop diseases that take decades to develop in humans.[10] This, in addition to the unique ability to alter the mouse genome by adding transgenes or altering endogenous genes, makes the mouse system an informative tool for understanding human disease.[9,10] The hundreds of inbred mouse strains, the more than 10,000 genetic markers mapped on mouse chromosomes, the ability to breed mice as desired, and the ability to maintain mice in highly controlled environments all enhance the strengths of the mouse system.[9] Genetic discoveries in mice often increase the understanding of human disease. For example, characterization of specific mutations in three mouse genes that cause different forms of retinal degeneration was rapidly followed by identification of the corresponding human genes as causes of

From the [1]Jackson Laboratory, Bar Harbor, Maine; [2]the Howard Hughes Medical Institute, Bar Harbor, Maine; [3]the Department of Ophthalmology, Tufts University School of Medicine, Boston, Massachusetts; [4]the Skirball Institute of Biomolecular Medicine, and Departments of Radiology and Pathology, New York University Medical Center, New York, New York; and [5]the Jules Stein Eye Institute, Los Angeles, California.

Supported by Jackson Laboratory startup funds and grants EY07758 and CA34196 from the National Institutes of Health, grant DBI 95-0221 from the National Science Foundation, and the Whitaker Foundation. Dan Turnbull is an Investigator of the American Heart Association-New York City Affiliate. Simon John is an Assistant Investigator of the Howard Hughes Medical Institute.

Submitted for publication October 24, 1997; accepted January 30, 1998.

Proprietary interest category: N.

Reprint requests: Simon John, the Jackson Laboratory, HHMI, 600 Main Street, Bar Harbor, ME 04609.

similar forms of retinal degeneration.[11-17] Additionally, it was mouse studies that led to the identification of apoptosis as an important mechanism of photoreceptor cell death in retinal degeneration.[18] The relatively poor understanding of the genetic and pathophysiological factors that cause glaucoma or alter glaucoma susceptibility highlights the need for mouse models of glaucoma.

We have identified a mouse model of hereditary glaucoma. As part of an ongoing program to identify mouse models of ocular disease, we noted pigment dispersion and obvious iris atrophy in 6- to 8-month-old mice of the inbred strain DBA/2J. Because pigment dispersion and iris atrophy with associated formation of anterior synechias can block aqueous drainage and cause human glaucoma,[19,20] we performed a clinical and histologic analysis of aging DBA/2J mice to determine whether they develop glaucoma. This article describes the development of pigment dispersion, iris atrophy, anterior synechias, and elevated IOP in DBA/2J mice. These changes are accompanied by retinal and optic nerve changes consistent with glaucoma. The disease progresses with increasing age, as does glaucoma in humans. This mouse strain is shown to exhibit elevated IOP, death of retinal ganglion cells, and atrophic excavation of the optic nerve, the hallmarks of glaucoma in humans.

Methods

Animal Husbandry

All experiments were performed in compliance with the ARVO Statement for Use of Animals in Ophthalmic and Vision Research. DBA/2J mice were housed in cages covered loosely with nonwoven polyester filters. The cages contained white pine bedding. The environment was kept at 21°C with a 14-hour light and 10-hour dark cycle. All mice were fed chow (6% fat; NIH31) ad libitum, and their drinking water was acidified to pH 2.8 to 3.2.

Clinical Examinations

The anterior chambers of mice ranging in age from 2 to 30 months were examined with a slit-lamp biomicroscope (Nikon, Tokyo, Japan). An indirect ophthalmoscope (American Optical, Rochester, NY) and a 60- or 90-diopter lens was used to visualize the retinas and optic nerves of mice between the ages of 2 and 30 months. For this analysis, pupils were dilated with a drop of 1% atropine sulfate.

Histologic Processing

Ocular Sections. Mice were euthanatized and eyes were immediately enucleated and fixed (0.8% paraformaldehyde and 1.2% glutaraldehyde in either 0.1 M phosphate buffer, pH 7.2, or 0.1 M cacodylate buffer, pH 7.2; adjusted to an osmolality of 840 to 930 mOsm).[21] After 24 to 48 hours, the fixative was replaced with the appropriate buffer. The eyes were processed by standard procedures and subsequently embedded in hydroxyethyl methylacrylate (Historesin, Leica, Heidelberg, Germany). We obtained serial sagittal sections (thickness of 1.5-3 μm) that passed through the optic nerve and included the pupil, and we cut 80 to 100 sections for most eyes. Analysis of these serial sections which included the width of the optic nerve, allowed us to accurately determine which sections came from the center of the nerve. Because the mouse optic nerve is small, it is important to have central sections to establish whether optic nerve cupping is present and to accurately assess its severity. Our experience indicates that it is easy to miss cupping or to misjudge its severity if central optic nerve sections are not obtained. Similarly it is important to estimate the retinal ganglion cell number at the same location in each eye, because the cell number varies widely with position. The identification of sections containing central optic nerve allowed us to do this. The sections were stained with hematoxylin and eosin, and the pathologic changes indicated below were assessed by analyzing these sections.

Optic Nerve Cross Sections. Mice were euthanatized at 3 and 18 months old. These animals were then decapitated, and most of the brain was removed from the skull, leaving a thin layer over the optic nerves. The heads were fixed by immersion as described above for the globes. After 24 to 48 hours, the fixative was replaced with buffer. Optic nerve regions extending from just in front of the optic chiasma to the back of the orbits were carefully dissected from the heads. The dissected nerves were postfixed with 1% osmium tetroxide and subsequently processed by standard procedures and embedded in a 1:1 epon-araldite mixture. Cross sections were cut from both ends of the tissue at a thickness of 250 nm and stained with Toluidine Blue O.

Definitions and Severity

All samples were analyzed by an investigator who was masked to the ages of the animals from which they were derived. In addition, to assess the reliability of severity designations for specific disease features, this investigator analyzed the eyes of 20 animals on two separate occasions while unaware of the animals' identities and ages. This is important because the assessment of severity was subjective and did not involve precise quantification. For both analyses, there was good agreement between the designated severities of specific features in any single eye.

The following are important definitions used in the Results and Discussion sections, and important notes relating to severity designations. The observed pathology relating to specific severity designations is explained in Table 1.

Donuts. This term describes thickening pupillary borders of the iris caused by the focal collection of cells filled with pigment. On clinical examination, the pupillary border often resembled a donut shape because it was thickened throughout its circumference. Donut severity was judged in relation to normal iris thickness and only at the pupillary border.

Peripheral Anterior Synechias. Peripheral anterior synechias are attachments of peripheral anterior iris to the trabecular meshwork and, in some cases to the peripheral posterior corneal surface.

Iris–Pigment Epithelium Atrophy. This is defined as a deterioration and loss of the iris pigment epithelium and atrophic thinning of the iris stroma.

Posterior Synechias. Posterior synechias are attachments of posterior iris surface to the anterior surface of lens. Severity was only estimated at or close to the pupillary border.

Ciliary Body Atrophy. Atrophy that involves vascular and epithelial layers of the ciliary processes and ciliary body.

Retinal Ganglion Cell Depletion. This is a visible loss of retinal ganglion cells. It is always estimated on a section that

TABLE 1. Grading Scheme for Ocular Lesions

*Lesion**	*Severity†*	*Observation*
Donuts	Mild	Pupillary border up to 2 NIT
	Moderate	Pupillary border thicker than 2 NIT but less than 4 NIT
	Severe	Pupillary border 4 NIT or greater
Peripheral anterior synechias	Mild	Only part of TM covered
	Moderate	Completely covers TM and very periphery of cornea
	Severe	Synechias extend more centrally onto the cornea
Iris—pigment epithelium atrophy	Mild	Iris stroma of normal thickness, fewer than normal iris pigment epithelium cells present
	Moderate	Stroma thinner than normal and few or no pigment epithelium cells present
	Severe	Stroma very thin (often thread-like) and no pigment epithelium present
Posterior synechias	Mild	Posterior iris barely attached to lens
	Moderate	Width of posterior iris attachment to lens was as wide as a typical iris sphincter muscle
	Severe	Width of iris to lens attachment greater than width of a typical iris sphincter and sometimes significantly larger
Ciliary body atrophy	Mild	Processes shortened but epithelium and vascular structures appear normal
	Moderate	Atrophic processes that have less distinct vascular and epithelial layers
	Severe	Atrophied to a flat epithelium without recognizable ciliary process structure
Retinal ganglion cell depletion	Normal	35–45 cells per 200×-magnified field
	Mild	20–30 cells per 200×-magnified field
	Moderate	10–20 cells per 200×-magnified field
	Severe	<10 cells per 200×-magnified field
Optic nerve atrophy	Mild	Estimated decrease in nerve diameter of no greater than 30% compared to a TN nerve
	Moderate	Estimated decrease in nerve diameter of 30%–60% compared to a TN nerve
	Severe	Estimated decrease in nerve diameter of greater than 60% compared to a TN nerve
Optic nerve cupping	Mild	Obvious cup present that extends no deeper than inner bipolar cell layer of retina
	Moderate	Cup extends to depth of outer bipolar cell layer
	Severe	Cup extends deeper than outer bipolar cell layer
	Gliotic	Degenerative pattern that resembles optic nerve cupping but the apparently cupped areas were filled with cells that are likely reactive glia

NIT, normal iris thickness; TM, trabecular meshwork; TN, typical normal.
*See Methods section for definitions.
†See Methods section for location at which severity was estimated.

includes the center of the optic nerve and at two optic disc diameters temporal to the optic nerve. The number of cells with large vesicular nuclei and abundant cytoplasm present in a 200× magnified field were estimated.

Optic Nerve Atrophy. Optic nerve atrophy is the disorganization and deterioration of normal nerve structure, including a decrease in nerve diameter. It is estimated in longitudinal central nerve sections attached to the posterior of the globe. As the severity of this atrophy increases, the axonal columns decrease in diameter.

Optic Nerve Cupping. This is defined as a thinning of the nerve fiber layer as it enters the optic nerve and atrophic excavation of the optic nerve. Severities were based on little if any physiological cup in mice and were only estimated in central optic nerve sections.

Intraocular Pressure Measurement

We measured IOPs directly using a microneedle system as previously described.[22] The pressure was recorded for a 1-minute period when the eye became stabilized after microneedle insertion. Mice of different ages were included in each measurement period as were C57BL/6J mice. The IOPs of C57BL/6J are consistent over time (unpublished observation) and so these animals were interspersed with experimental mice to ensure that calibration had not drifted and that the system was functioning optimally.

TABLE 2. Histology Findings in DBA/2J Mice

Age (months)	*Donuts*	*I–PEA*	*PAS*	*PS*	*CBA*	*Lens*	*RGCD*	*ONA*	*ONC*
6-7	3/3*	6/6	4/6	2/3	3/6	0/6	0/6	0/3	0/3
	2 mi†	*5 mi*	*4 mi*	*1 mi*	*3 mi*				
	1 mo	*1 sev*		*1 mo*					
8-9	20/20	22/22	21/22	18/19	11/22	0/20	0/20	1/18	0/17
	4 mi	*3 mi*	*11 mi*	*1 mi*	*9 mi*			*1 mo*	
	14 mo	*15 mo*	*9 mo*	*14 mo*	*2 mo*				
	2 sev	*4 sev*	*1 sev*	*3 sev*					
11-15	14/16	26/26	26/26	18/19	24/26	3/26	51/6	9/16	2/11
	4 mi	*2 mi*	*2 mi*	*3 mi*	*7 mi*	*1 NC*	*5 mi*	*5 mi*	*1 mi*
	8 mo	*10 mo*	*16 mo*	*11 mo*	*15 mo*	*2 NCC*		*4 mo*	*1 mo*
	2 sev	*14 sev*	*8 sev*	*4 sev*	*2 sev*				
18-19	3/20	21/21	21/21	17/20	21/21	16/21	14/19	15/22	3/13
	2 mi	*1 mo*	*10 mo*	*3 mi*	*1 mi*	*7 CC*	*7 mi*	*3 mi*	*3 gl*
	1 sev	*20 sev*	*11 sev*	*7 mo*	*6 mo*	*8 NCC*	*7 mo*	*10 mo*	
				7 sev	*14 sev*	*1 ASC, PSC, CC*		*2 sev*	
20-22	2/11	15/15	15/15	12/12	15/15	5/13	8/11	10/11	4/6
	1 mi	*2 mo*	*6 mo*	*1 mi*	*5 mo*	*4 CC*	*3 mi*	*1 mi*	*2 mo*
	1 mo	*13 sev*	*9 sev*	*2 mo*	*10 sev*	*1 NCC*	*4 mo*	*2 mo*	*1 mi*
				9 sev			*1 sev*	*7 sev*	*1 gl*

I-PEA, iris-pigment epithelium atrophy; PAS, peripheral anterior synechias; PS, posterior synechias; CBA, ciliary body atrophy; RGCD, retinal ganglion cell depletion; ONA, optic nerve atrophy; ONC, optic nerve cupping; CC, cortical cataract; NCC, nuclear cortical cataract; ASC, anterior subcapsular cataract; PSC, posterior subcapsular cataract; *mi,* mild; *mo,* moderate; *sev,* severe, and *gl,* gliotic.

*The numerator indicates the number of eyes exhibiting the lesion, whereas the denominator indicates the number of eyes successfully analyzed for that lesion.

†The number of eyes with a finding of a specific severity is shown in *italics.* The severity of each finding was determined by consensus after inspection of multiple sections. The presence, absence, or severity of specific changes was only assessed at specific ocular locations (see Methods section). The number of eyes successfully analyzed for each finding varies because pupillary or central optic nerve sections were not always obtained or because artifacts obscured specific features. The severity of specific abnormalities is variable within each age group. Nevertheless, the age groups are arranged so that overall prevalence or severity of disease features within a particular group was not obviously different between the youngest and oldest animals in that group. None of these changes were observed on histologic analysis of the eyes of eight mice that were between 3 and 5 months of age. Data for mice older than 22 months are not shown because only a few eyes were successfully analyzed, and they were not obviously different from the eyes of 22-month-old mice.

lium and contained fine vascular channels (Fig. 2J). By the age of 11 to 15 months, the ciliary processes usually became flattened, as did the underlying ciliary body, and vascular channels were less evident (Fig. 2K). In the late stages of glaucoma, the ciliary body and processes underwent further atrophy (Fig. 2L).

Retina. The retinas of young DBA/2J mice had normal morphologic features that were similar to those in other mouse strains. Specifically, the retinal ganglion cell layer consisted of one to two layers of cells characterized by vesicular nuclei and prominent nucleoli, and a thin nerve fiber layer ran along the inner retinal surface. The bipolar cell layer was six to eight cells thick (Fig. 3A). (For simplicity, we refer to the inner nuclear layer as the bipolar cell layer.) As glaucoma developed, the nerve fiber layer became thinner and a single layer of sparse ganglion cells was evident (Fig. 3B). In advanced cases, the number of normal-appearing ganglion cells was greatly depleted (Fig. 3C). The ganglion cell layer was the most susceptible to cell loss, which appeared to increase with age. However, in some cases significant retinal thinning did occur, and the bipolar cell layer was sometimes reduced to a thickness of three to four cells (Fig. 3C).

Optic Nerve. In the young DBA/2J optic nerve, the lamina cribrosa was easily identified, and broad nerve fiber columns were separated by delicate fibrovascular pial septae (Fig. 3D). By 11 months, optic nerve atrophy and disorganization was evident in approximately half of the animals. By 18 to 22 months, the lamina cribrosa could no longer be defined in most animals, the nerve fiber columns had typically collapsed, and the pial septae were usually irregular (Fig. 3E). In severe cases, the optic nerve was sometimes less than 25% of the diameter of a normal nerve, and the nerve fiber columns had disappeared. There was also an extensive increase in cellularity per unit area of nerve that might have reflected glial proliferation (compare Fig. 3D with Fig. 3F).

In young mice, a thick peripapillary nerve fiber layer formed the optic nerve, usually with no obvious physiological cup. Elements of the lamina cribrosa extended from the level of the retinal pigment epithelium nearly to the posterior edge of the sclera (Fig. 3G). As glaucoma progressed with age, optic nerve cupping developed in some but not all eyes. Some eyes exhibited severe optic nerve atrophy but no cupping. Mild cupping of the optic nerve involving thinning of the peripapillary nerve fiber layer and atrophic excavation extending to the depth of the inner bipolar cell layer was present in some animals by 11 months of age (Fig. 3H). The prevalence of cupping appeared to increase with age (Table 2). In some advanced cases, cupping extended posterior to the depth of the outer bipolar cell layer (Fig. 3I).

A limited study, involving two mice of each age, sug-

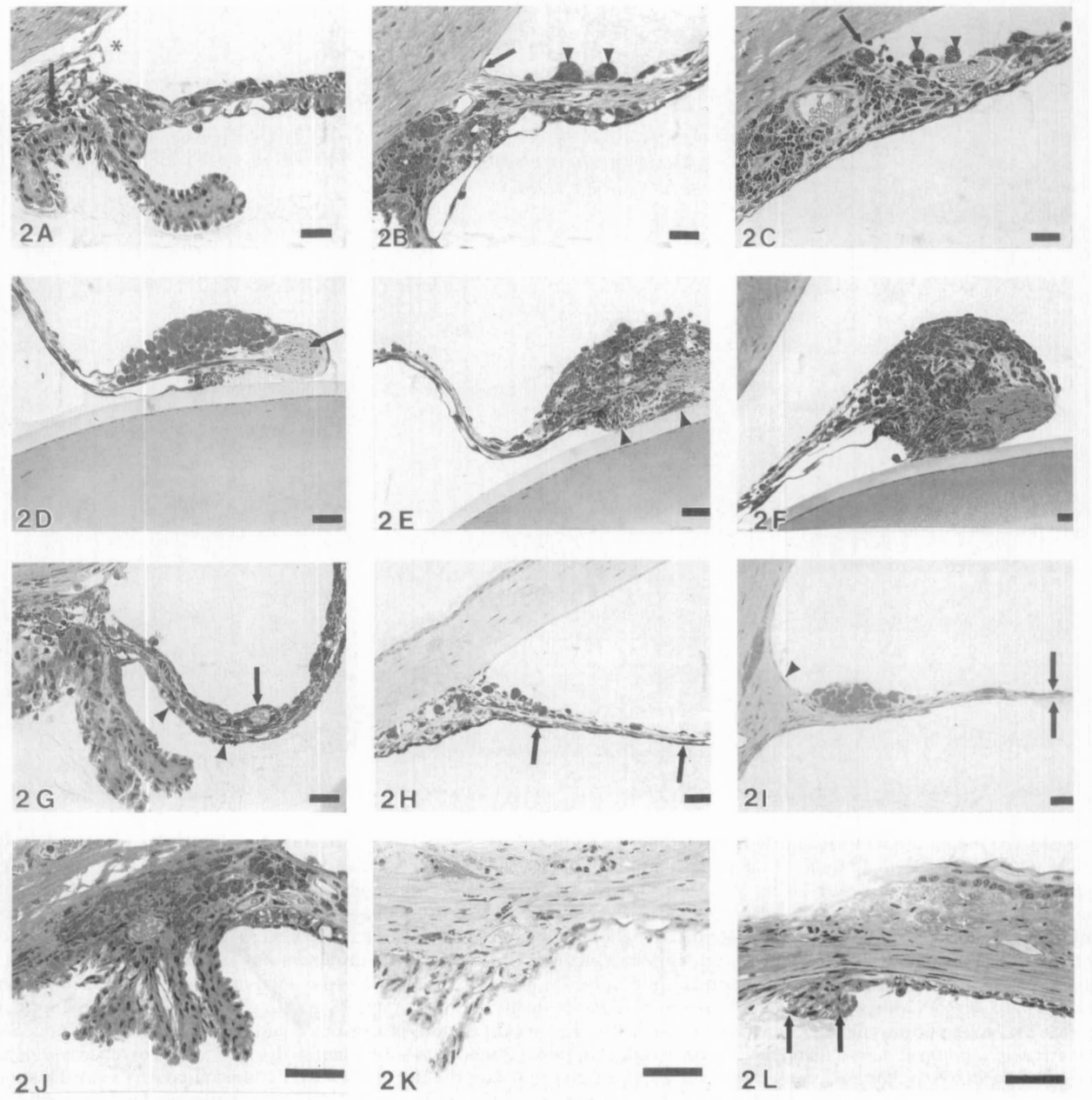

FIGURE 2. Anterior segment abnormalities in DBA/2J mice. The panels are arranged to represent the progressive increase in severity from *left* to *right*. **(A)** Young DBA/2J mouse. The anterior chamber angle is open (*). An occasional clump cell is present at the iris root (*arrow*). **(B)** Moderate anterior synechias, with angle closure (*arrow*). Pigment-filled macrophages are abundant in the iris root, and some are present on the anterior iris surface (*arrowheads*). **(C)** Severe anterior synechias obstruct the angle structures and extend centrally onto the cornea (*arrow*). Numerous pigment-filled macrophages are present on the iris surface (*arrowheads*) and in the iris root. **(D)** Early donut. A collection of pigmented macrophages lies anterior to the sphincter (*arrow*). **(E)** A moderate donut is present, and posterior synechias (*arrowheads*) attach the iris to the lens capsule. **(F)** Severe donut. **(G)** Young DBA/2J mouse. Iris vessels (*arrow*) are present. The posterior pigmented epithelium (*arrowheads*) is normal. **(H)** Moderately advanced iris atrophy. The two layers of iris epithelium can no longer be identified, although a thin line of flattened pigment cells remains (*arrows*). **(I)** Severe iris atrophy. The iris is reduced to a thread-like structure (*double arrows*) without identifiable iris pigment epithelium. The angle recess is covered by endothelial cells and Descemet's membrane-like material (*arrowhead*). **(J)** Young DBA/2J ciliary body. Four ciliary processes are identified with well-defined ciliary epithelium and central vascular channels. **(K)** Moderate ciliary body atrophy. Fewer ciliary processes are present, and they are shorter and narrower than those illustrated in J. **(L)** Severe ciliary body atrophy. Severely flattened ciliary processes without vascular channels are barely identifiable (*arrows*). Scale bar, 100 μm.

gests that the age-related increase in retinal ganglion cell death and optic nerve atrophy was usually paralleled by a marked reduction in the number of myelinated nerve fibers in the proximal optic nerve. In the proximal optic nerve of 3-month-old DBA/2J mice, the individual myelin sheaths were tightly packed and the majority were of small diameter. In contrast, in 19-month-old DBA/2J optic nerves there was a marked reduction in the number of nerve fibers (Fig.

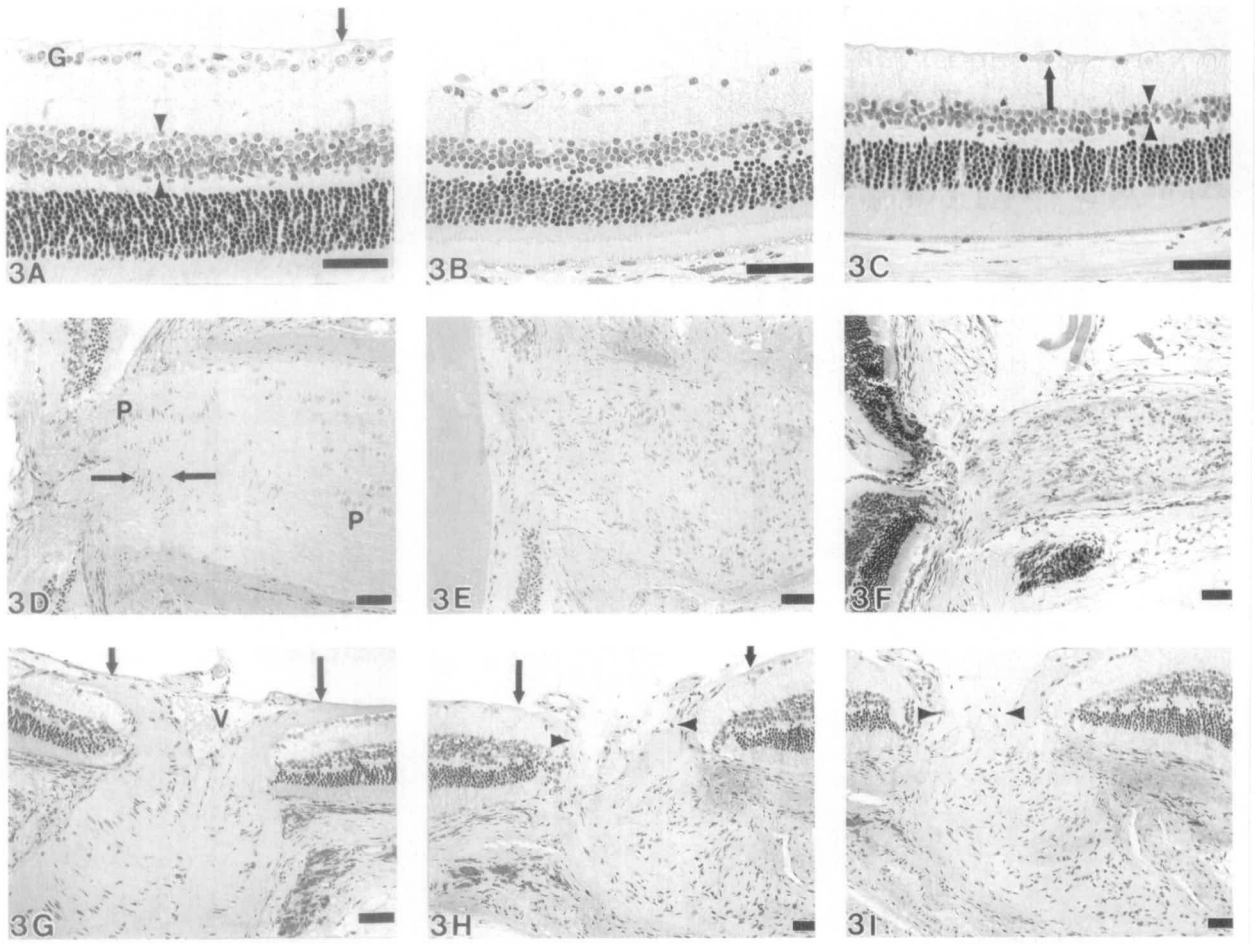

FIGURE 3. Glaucomatous abnormalities in DBA/2J mice. The panels are arranged to represent the progressive increase in severity from *left* to *right*. (**A**) Normal retina, young DBA/2J mouse. There is a delicate nerve fiber layer (*arrow*), one to two layers of retinal ganglion cells (G), and six to eight layers of bipolar cells (*arrowheads*). (**B**) Moderately advanced glaucoma. The nerve fiber layer cannot be identified. Retinal ganglion cells are diminished in number and reduced to a single layer. There is a suggestion of thinning of the bipolar layer. (**C**) Severe glaucoma. Retinal ganglion cells (*arrow*) are scarce. The darker staining nuclei are either dying ganglion cells or vascular endothelial cells. The bipolar cell layer (*arrowheads*) is three to four cells thick, and there may be a modest loss of photoreceptor cells. (**D**) Normal optic nerve, young DBA/2J mouse. Horizontal elements of the lamina cribrosa (between *arrows*) are easily visualized. Nerve fiber columns are distinct and separated by pial septae (P). (**E**) Moderate optic nerve atrophy. The lamina cribrosa is no longer well defined. The nerve columns are disorganized and less distinct. (**F**) Advanced optic nerve atrophy. The optic nerve diameter is greatly reduced, nerve fibers cannot be identified, and there is extensive gliosis. (**G**) Optic nerve head, young mouse. As the nerve fibers approach the nerve, the nerve fiber layer is thickened (*arrows*). This section passes through a central retinal vessel (V), but there is no true cupping of the nerve. (**H**) Early cupping. The nerve fiber layer (*arrows*) has become thin as it enters the nerve. Cupping extends to the anterior layer of bipolar cells (*arrowheads*). (**I**) Advanced cupping. The nerve fiber layer cannot be identified. Cupping extends to the posterior aspect of the bipolar cell layer (*arrowheads*). Scale bar, 100 μm.

4). Interestingly, many of the remaining nerve fibers had large diameters (estimated to be 2 to 10 times those of the majority of nerve fibers in young mice).

Intraocular Pressure

IOP was measured at ages 3, 6, 9, and 19 months (Fig. 5). Multifactorial analysis of variance (excluding the data for 19 months because only males were analyzed at this age) showed that age and sex had significant effects on IOP (age, $P < 0.0001$; sex, $P = 0.015$). In the following results, mean IOPs are reported ± standard error of the mean, and the P values are from post hoc Fisher least significant difference tests.

The IOPs of 3-month-old males and females showed no significant differences ($P = 0.7$). Regarding increasing age, there were no significant differences in IOP between either 3 and 6 month old males or between 3 and 6 month old females ($P = 0.2$ in both cases). Nevertheless, the IOPs of some 6-month-old females were considerably higher than those of the males, and there was a significant difference between the IOP distributions of each sex at this age (males, mean 9.4 ± 0.4 mm Hg, median 9.3 mm Hg; females, mean 13 ± 0.9 mm Hg, median 11.3 mm Hg; $P = 0.03$). The IOP distributions of male and female mice shifted upward by 9 months ($P < 0.0001$ for 6 versus 9 months in both cases), and the sex difference was still evident (males, mean 16.2 ± 1.4 mm Hg, median 14.1 mm Hg; females, mean 20.3 ± 1.8 mm Hg, median 19.7 mm Hg; $P = 0.003$). Only males were analyzed at 19 months old. By this age, the IOPs of most males had decreased to low levels (mean 5.7 ± 0.6 mm Hg; median 4.9 mm Hg).

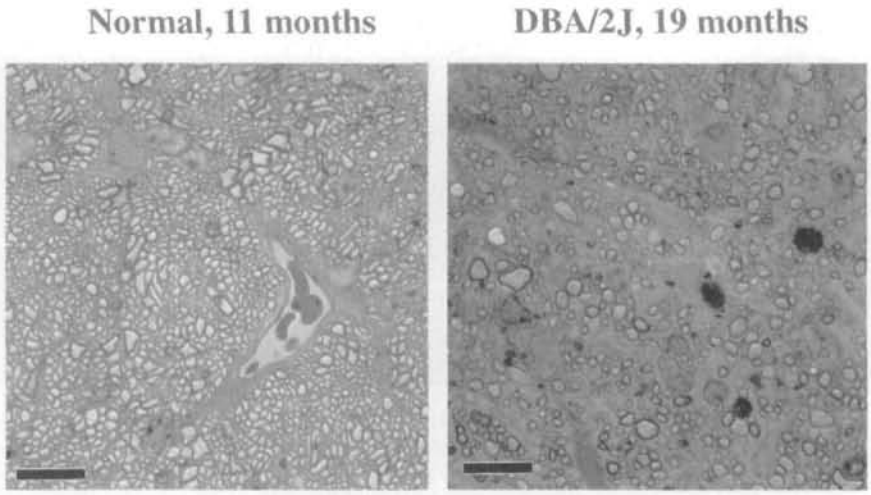

FIGURE 4. Axonal changes in the optic nerve. Images of representative areas within optic nerve cross sections of two mice of the indicated ages. DBA/2J nerves from mice aged 3 months are similar to the normal nerve from a strain 129/J mouse. The axon number is greatly decreased in the glaucomatous 19-month-old DBA/2J nerve. The axonal loss in this nerve reflects the significant decrease in retinal ganglion cells observed in saggital sections through the corresponding eye. Scale bar, 10 μm.

Anterior Chamber Depth

A few aging DBA/2J mice had obviously enlarged bulging eyes. After withdrawal of the microneedle (and aqueous humor leakage) subsequent to IOP measurement, the corneas of these eyes were loose and wrinkled. This suggested that the anterior chambers had enlarged as a consequence of aqueous accumulation. Additionally, microscopic viewing during IOP assessment suggested that the anterior chambers of most aging DBA/2J mice were deeper than those of younger mice. (Young DBA/2J mice were similar to young and old mice of other mouse strains that do not develop iris atrophy and synechias.) Therefore, we devised a procedure to analyze the anterior chambers of living mice using UBM. This procedure was then used to generate image data for measurement of anterior chamber depth in both eyes of mice of different ages (Fig. 6). In most eyes, anterior chamber depth increased dramatically with age ($P < 0.001$ by analysis of variance). The average chamber depth increased from 323 ± 51 μm (mean ± SEM) at 2 months (8 eyes) to 519 ± 51 μm at 9 months (8 eyes) and to 648 ± 42 μm at 13 months (10 eyes). This was the case in right and left eyes, and all analyzed DBA/2J eyes were enlarged at 13 months.

Other Findings

Corneal calcification occurred in many eyes. Its incidence and severity increased with age. A number of old mice (24 months or older) had corneal ulcers that appeared to result from foreign body reactions after deterioration of the corneal epithelium. Because of the inflammatory response, these eyes were excluded from our analyses. In some ocular sections, a substance resembling protein was present in the anterior chamber. Nuclear cataracts and subcapsular cataracts (involving epithelial proliferation and migration) occurred with increased frequency and severity in old animals. In severe cases, the lens was swollen. Posterior displacement of the lens occurred in a few old animals that had severe ciliary body atro-

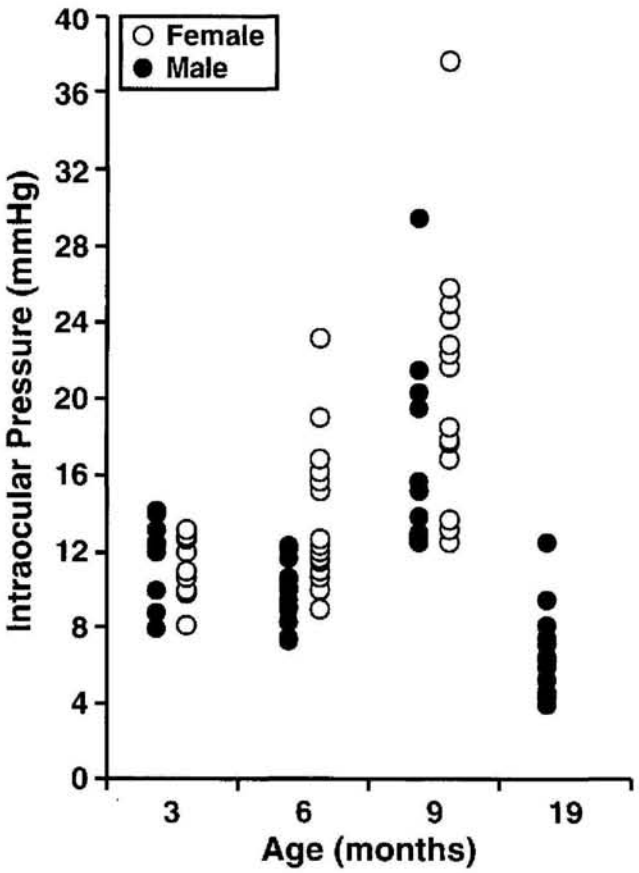

FIGURE 5. Intraocular pressure (IOP) as a function of age and sex. IOPs of individual mice of the indicated ages are shown. The number of males (M) and females (F) successfully analyzed at 3, 6, 9, and 19 months were: M3, 9; F3, 10; M6, 14; F6, 20; M9, 14; F9, 14; M19, 16.

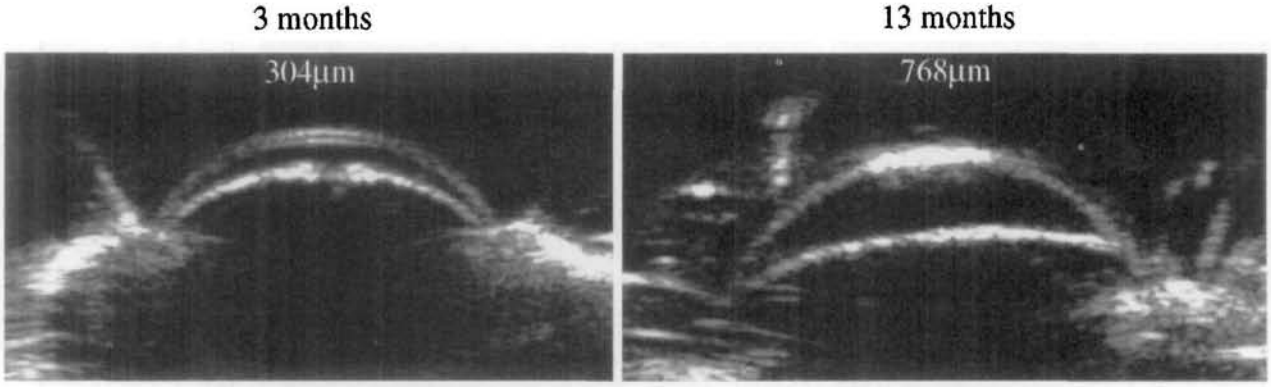

FIGURE 6. Anterior chamber depth increases with age. Ultrasound images at the deepest point of the anterior chambers of DBA/2J mice of the indicated ages. The numbers refer to the maximal depth of each chamber. The chamber depth in DBA/2J mice increases dramatically with age. Central corneal scarring is also evident in the 13-month-old DBA/2J mouse.

phy. In these cases, the zonules appeared to be relaxed. Gross examination of enucleated eyes from animals 18 months or older revealed loss of choroidal pigment.

DISCUSSION

This study documented the development of anterior segment anomalies that resulted in an elevation of IOP and caused glaucoma in mice of the DBA/2J strain. This mouse strain is inbred; hence, all individuals of this strain are genetically identical (except for their sex chromosomes). We were careful to keep the environments similar between cages and over time. The severity of specific changes was assessed only at precise ocular locations. Despite this, there was significant variability in the age of onset and the severity of specific lesions within and between animals, as seen in glaucoma in humans. This variability suggests that subtle environmental differences, stochastic effects, or both modify the phenotype. Despite phenotypic variability, glaucoma develops in nearly all eyes, and the disease follows a predictable progressive path. The majority of mice suffer loss of retinal ganglion cells and optic nerve atrophy by 22 months of age (Table 2). This consistency in glaucoma development suggests that it is feasible to use this mouse strain to assess the mechanisms affecting cell death in glaucoma and to characterize genes that alter susceptibility to glaucomatous nerve damage.

Clinically, the first identifiable signs are transillumination defects of the peripheral iris that involve pigment dispersion and iris thickening at the pupillary border caused by the localized collection of pigment-filled macrophages. These changes are first noted between the ages of 3 and 4 months and become more severe with time (Fig. 1). Iris stromal atrophy is apparent in some animals by 6 months and increases progressively.

Histologic analysis of DBA/2J eyes generally agrees well with the clinical analysis. However, histologic studies detected no abnormalities in approximately eight eyes from mice that were 3 to 5 months old, and there was no detectable sex difference in the age of onset of iris abnormalities. These differences are likely explained by the finding that early pathologic changes were not extensive and tended to be focal. It is reasonable to assume that focal changes detected on clinical examination were not present in the histologic sections that only included a small portion of the eye. (Even though sections containing the entire width of the optic nerve were included in our histologic analysis, these sections still represent only a small portion of the eye).

Many DBA/2J mice develop elevated IOP (Fig. 5). Several disease features may account for this. Iris pigment dispersion and iris atrophy are accompanied by the accumulation of pigment-filled macrophages in the anterior chamber angle and the development of peripheral anterior synechias (Fig. 2). In some eyes, flattened cells that resembled corneal endothelial cells extended across the surface of the anterior synechias and onto the anterior surface of the peripheral iris. These changes could impede the drainage of aqueous humor and result in elevated IOP. Similarly, the thickening of the iris pupillary border caused by macrophage accumulation and the development of posterior synechias (Fig. 2) could inhibit the flow of aqueous humor from the posterior chamber to the anterior chamber and contribute to increased IOP.

IOP tends to increase earlier in females than in males. At 6 months, the IOP of most males is similar to that at 3 months; however, a number of 6-month-old females have considerably elevated IOP (Fig. 5). In fact, as a group, females have significantly higher IOPs than males at this age ($P = 0.03$). (It is noteworthy that females also tend to develop iris transillumination defects and iris atrophy earlier than males.) Even though the IOPs of both sexes increase by 9 months, this is true for a greater proportion of females than males, and a significant difference in the IOP distributions of both sexes still exists at this age ($P = 0.003$). This suggests that female outflow is more severely compromised than male outflow, even though there are no obvious histologic differences between the sexes at this age. By 19 months, the IOPs of many male mice have decreased to low levels (19-month-old females were not assessed). This likely results from severe ciliary body atrophy that is evident in the majority of animals by this age (Table 2, Fig. 2). Because no sex differences were detected for ciliary body atrophy, it is reasonable to expect that the IOP of females is also low by 19 months. To determine the age at which the IOP peaks in most eyes, the magnitude of peak IOPs, and the age at which IOP starts to decline, it is necessary to determine the IOPs of mice of both sexes at more time points between the ages of 9 and 19 months.

The anterior segment changes and consequent IOP elevation are followed by retinal ganglion cell death, optic nerve

atrophy, and cupping of the optic nerve (Fig. 3, Table 2). Taken together, these findings lead to a diagnosis of secondary angle-closure glaucoma. The severity of the retinal and optic nerve changes was variable at any particular age, as was their age of onset. This variability probably is related to variability in the severity and age of onset of the anterior segment anomalies and to variability in the magnitude and duration of IOP elevation in specific eyes. Because of technical limitations, we have not analyzed the relationship between retinal and optic nerve damage and the magnitude and duration of IOP elevation. We are developing equipment for noninvasive IOP measurement in mice that will facilitate such studies.

Ocular abnormalities were previously reported in mice of various DBA/2 substrains.[26-28] These reports noted a number of the features identified in this study, including corneal opacities, cataracts, iris atrophy, and anterior synechias. Retinal ganglion cell death and optic nerve atrophy were recently reported in the DBA/2NNia substrain.[28] Though similar, the disease documented in the DBA/2NNia substrain differs in several respects from that characterized here in DBA/2J mice. For example, cupping of the optic nerve was not observed in DBA/2NNia mice (up to 24 months old), whereas prominent cupping is frequently observed by 22 months in DBA/2J mice (Table 2, Fig. 3). Additionally, the age of onset and the incidence of various ocular abnormalities vary dramatically among different reports. These may be explained by differences in the methods of evaluation, environment, or substrain used.

The progressive ocular changes that develop in DBA/2J mice are similar to those found in specific glaucoma syndromes in humans.[29-32] The disease in DBA/2J mice resembles a mixture of pigment dispersion syndrome and the iridocorneal endothelial syndrome. Pigment dispersion syndrome involves a dispersal of iris pigment that is deposited in the aqueous outflow pathway.[29] The changes observed clinically in young DBA/2J mice strongly resemble pigment dispersion syndrome. However, unlike the disease in DBA/2J mice, pigment dispersion syndrome is usually associated with open-angle glaucoma and does not involve large accumulations of pigment-filled cells or synechia. The iridocorneal endothelial syndrome is a complex of three previously described syndromes with overlapping clinical findings—essential iris atrophy, Chandler's syndrome, and the iris nevus syndrome.[30-32] Glaucoma is associated with all these syndromes in some cases. Some of the features of iridocorneal endothelial are evident in DBA/2J mice. Essential iris atrophy is characterized by prominent iris atrophy accompanied by pupillary distortion and corectopia. Anterior synechia formation is a late complication that may be preceded by glaucoma. The iris changes in DBA/2J mice closely resemble those occurring in essential iris atrophy. (In Chandler's syndrome, the iris atrophy is less evident and corneal edema is a common occurrence.) The iridocorneal endothelial syndrome also is characterized by endothelization of the angle and anterior iris. Endothelization of the anterior synechias and anterior iris occurred in some DBA/2J mice.

In summary, we have documented the development of a progressive disease involving iris atrophy, pigment dispersion, and glaucoma in aging DBA/2J mice. The availability of this mouse model of glaucoma will allow further research to delineate the genetic and pathophysiological basis of retinal and optic nerve damage in the face of elevated IOP and may provide a basis for the evaluation of therapeutic modalities in glaucoma therapy.

Acknowledgments

The authors thank John Sundberg for his help, support, and critical reading of this manuscript; Deborah Boswell-Lane and other members of The Jackson Laboratory Biological Imaging Service; Jane Przyborski, Beth Whitney, Janice Buckingham, Jennifer Smith, and Joyce Worcester for their assistance; and Tim O'Brien for critical reading of the manuscript.

References

1. Thylefors B, Negrel AD. The global impact of glaucoma. *Bull World Health Organ.* 1994;72:323-326.
2. Leske MC. The epidemiology of open-angle glaucoma: a review. *Am J Epidemiol.* 1983;118:166-191.
3. Shields MB. *Textbook of Glaucoma.* Baltimore: Williams & Wilkins; 1992.
4. Shields MB. Primary open-angle glaucoma. In: *Textbook of Glaucoma.* Baltimore: Williams & Wilkins; 1992:172-197.
5. Fatt I, Weissman BA. *Physiology of the Eye: An Introduction to the Vegetative Functions.* Boston: Butterworth-Heinemann; 1992.
6. Sarfarazi M. Recent advances in molecular genetics of glaucomas. *Hum Mol Genet.* 1997;6:1667-1677.
7. Stone EM, Fingert JH, Alward WLM, et al. Identification of a gene that causes primary open angle glaucoma. *Science.* 1997;275:668-678.
8. Stoilov I, Akarsu AN, Sarfarazi M. Identification of three different truncating mutations in cytochrome P4501B1 (CYP1B1) as the principal cause of primary congenital glaucoma (Buphthalmos) in families linked to the GLC3A locus on chromosome 2p21. *Hum Mol Genet.* 1997;6:641-647.
9. Paigen K. A miracle enough: the power of mice. *Nat Med.* 1995; 1:215-220.
10. Smithies O, Maeda N. Gene targeting approaches to complex genetic diseases: atherosclerosis and essential hypertension. *Proc Natl Acad Sci USA.* 1995;92:5266-5272.
11. Travis GH, Brennan MB, Danielson PE, Kozak CA, Sutcliffe JG. Identification of a photoreceptor-specific mRNA encoded by the gene responsible for retinal degeneration slow (rds). *Nature.* 1989;338:70-73.
12. Bowes C, Li T, Frankel WN, et al. Localization of a retroviral element within the rd gene coding for the beta subunit of cGMP phosphodiesterase. *Proc Natl Acad Sci USA.* 1993;90:2955-2959.
13. Pittler SJ, Baehr W. Identification of a nonsense mutation in the rod photoreceptor cGMP phosphodiesterase beta-subunit gene of the rd mouse. *Proc Natl Acad Sci USA.* 1991;88:8322-8326.
14. Weil D, Blanchard S, Kaplan J, et al. Defective myosin VIIA gene responsible for Usher syndrome type 1B. *Nature.* 1995;374:60-61.
15. Gibson F, Walsh J, Mburu P, et al. A type VII myosin encoded by the mouse deafness gene shaker-1. *Nature.* 1995;374:62-64.
16. Kajiwara K, Hahn LB, Mukai S, et al. Mutations in the human retinal degeneration slow gene in autosomal dominant retinitis pigmentosa. *Nature.* 1991;354:480-483.
17. McLaughlin ME, Sandberg MA, Berson EL, Dryja TP. Recessive mutations in the gene encoding the beta-subunit of rod phosphodiesterase in patients with retinitis pigmentosa. *Nat Genet.* 1993;4:130-134.
18. Chang GQ, Hao Y, Wong F. Apoptosis: final common pathway of photoreceptor death in rd, rds, and rhodopsin mutant mice. *Neuron.* 1993;11:595-605.
19. Shields MB. Glaucomas associated with disorders of the iris. In: *Textbook of Glaucoma.* Baltimore: Williams & Wilkins; 1992:276-286.
20. Shields MB. Glaucomas associated with disorders of the corneal endothelium. In: *Textbook of Glaucoma.* Baltimore: Williams & Wilkins; 1992:258-275.
21. Smith RS, Rudt LA. Ultrastructural studies of the blood-aqueous barrier 2: the barrier to horseradish peroxidase in primates. *Am J Ophthalmol.* 1973;76:937-947.
22. John SWM, Hagaman JR, MacTaggart TE, Peng L, Smithes O. Intraocular pressure in inbred mouse strains. *Invest Ophthalmol Vis Sci.* 1997;38:249-253.

23. Turnbull DH, Starkoski BG, Harasiewicz KA, et al. A 40-100 MHz B-scan ultrasound backscatter microscope for skin imaging. *Ultrasound Med Biol.* 1995;21:79-88.
24. Turnbull DH, Bloomfield TS, Baldwin HS, Foster FS, Joyner AL. Ultrasound backscatter microscope analysis of early mouse embryonic brain development. *Proc Natl Acad Sci USA.* 1995;92:2239-2243.
25. Pavlin C, Foster F. *Ultrasound Biomicroscopy of the Eye.* New York: Springer-Verlag; 1995.
26. Epstein RJ, Halkias A, Stulting DR, Rodrigues MM. Corneal opacities and anterior segment anomalies in DBA/2 mice: possible models for corneal elastosis and the iridocorneal endothelial (ICE) syndrome. *Cornea.* 1986;5:95-105.
27. Bronson RT, Lipman RD. Reduction in rate of occurrence of age related lesions in dietary restricted laboratory mice. *Growth Dev Aging.* 1991;55:169-184.
28. Sheldon WG, Warbritton AR, Bucci TJ, Turturro A. Glaucoma in food-restricted and ad libitum-fed DBA/2NNia mice. *Lab Anim Sci.* 1995;45:508-518.
29. Scheie HG, Cameron JD. Pigment dispersion syndrome: a clinical study. *Br J Ophthalmol.* 1981;65:264-269.
30. Lichter PR. The spectrum of Chandler's syndrome: an often overlooked cause of unilateral glaucoma. *Ophthalmology.* 1978;85:245-251.
31. Shields MB. Progressive essential iris atrophy, Chandler's syndrome, and the iris nevus (Cogan-Reese) syndrome: a spectrum of disease. *Surv Ophthalmol.* 1979;24:3-20.
32. Spencer WH. Glaucoma. In: Spencer WH, ed. *Ophthalmic Pathology: An Atlas and Textbook.* Philadelphia: WB Saunders; 1996:438-512.